Dynamics of clay-intercalated Ibuprofen studied by Solid State NMR

Elisa Carignani[¥,‡,*], *Silvia Borsacchi*[‡], *Paolo Blasi*[§], *Aurélie Schoubben*[§], *Marco Geppi*[¥,‡,*]

[¥] Dipartimento di Chimica e Chimica Industriale, Università di Pisa, via G. Moruzzi 13, 56124 Pisa, Italy

[‡] Istituto di Chimica dei Composti Organo Metallici − CNR, via G. Moruzzi 1, 56124 Pisa, Italy

[§] Dipartimento di Scienze Farmaceutiche, Università di Perugia, via del Liceo 1 – 06123 Perugia, Italy

[$]Scuola di Scienze del Farmaco e dei Prodotti della Salute, Università di Camerino, via S. Agostino 1 – 62032 Camerino, Italy

KEYWORDS: drug delivery systems, pharmaceutical formulations, clay, MAS NMR, nuclear relaxation.

TABLE OF CONTENTS/ABSTRACT GRAPHIC

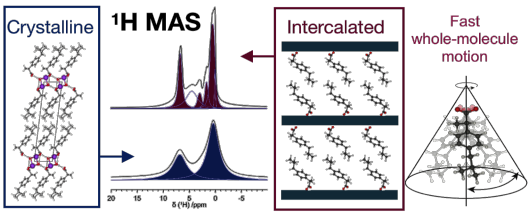

ABSTRACT: In designing drug formulations with improved release properties and bioavailability the dynamic features of the active pharmaceutical ingredient can be crucial for the final product properties. In this work we aimed at obtaining the first characterization of the molecular dynamic properties of one of the most common non steroidal anti-inflammatory drug, Ibuprofen, intercalated in hydrotalcite, an interesting inorganic carrier. By exploiting a variety of Solid State NMR techniques, including ^{1}H and ^{13}C MAS spectra and T_1 relaxation measurements, performed at variable temperature, and carrying out a synergic analysis of all results it has been possible to ascertain that the mobility of Ibuprofen within the carrier is remarkably increased. In particular, strong indications have been obtained that Ibuprofen molecules, in addition to internal interconformational dynamics, experience an overall molecular motion. Also considering that Ibuprofen is "anchored" to the charged surface of the hydrotalcite layers through its carboxylate moiety, such motion could be a *wobbling-in-a-cone*. Activation energies and correlation times of all the motions of intercalated Ibuprofen have been determined.

INTRODUCTION

Solid oral dosage forms are the leading marketed formulations because of the superior patient compliance and the higher active pharmaceutical ingredient (API) stability. Virtually, no API possesses adequate characteristics to be administered on its own. This makes necessary the combination of APIs with other materials (i.e., excipients) and the use of *ad hoc* technological procedures (i.e., formulation) to confer them the required features to be dispensed through the selected route. Once the medical product is administered to patients, the API has to be dissolved and released in the body fluids to be absorbed and distributed to all the organs and tissues. Since

immediate release solid oral dosage forms still account for a large majority of prescriptions, solubility and dissolution rate have a fundamental role in biopharmaceutics. Many molecules approved or in the pipeline have a low - or very low - solubility in water and physiological media, thus creating bioavailability issues that compromise the desired therapeutic effect.[1]

The need to deliver efficiently poorly water-soluble compounds in the body has stimulated academia and industry to develop formulation strategies to improve the dissolution rate and/or solubility/apparent solubility of poorly water-soluble drugs. One of the promising strategies currently under investigation is the use of porous (e.g., mesoporous silica)[2] or lamellar (e.g., hydrotalcite-like compounds)[3] inorganic materials able to host APIs in a non-crystalline form or in crystalline state. Being in an amorphous or molecularly dispersed form, APIs show an increased dissolution rate with a consequent increase of their bioavailability.

Hydrotalcite-like compounds, also known as layered double hydroxides are a family of anionic clays, with formula $[M(II)_{1-x}\, M(III)_x\, (OH)_2\,]^{x+}\, [A_{x/n}{}^{n-}\,]^{x-}\, m\, S$. The clay layers are constituted by divalent (*M(II)*) and trivalent (*M(III)*) metal cations (generally Mg and Al), occupying the centres of octahedra with hydroxide ions at the vertices. The layers have a positive charge, which is balanced by exchangeable anions A^{n-}. S is a co-intercalated solvent, usually water. These clays possess a series of favourable characteristics for their use as excipients in pharmaceutical technology. Some of them (e.g., Mg-Al-hydrotalcite, Mg-Al-HTlc) are already employed in pharmaceutics and drug delivery.[4,5] They have not raised toxicity concerns, are easy to synthesize as micro- or nano-sized crystals, and can be loaded with different types of API, from small molecules to nucleic acids, that are easily intercalated in the inter-layer galleries of the clay.[6,7,8] One very promising feature of layered solids intercalating guest molecules is their ability to release the guest molecules with different kinetics in different physiological media.[9]

Since the release of guest molecules, but also the performances of the system (API intercalated in the layered solid), may be strongly affected by the structure of the complex, the arrangement of the API, and also its dynamics within the clay galleries, a deep understanding of these properties is highly desirable.

Ibuprofen, an important non-steroidal anti-inflammatory drug, is one of the most commonly administered APIs in the world and is also often used as model compound in scientific studies since the polymorphism and structural properties of its acid[10,11,12] and sodium forms[13,14] have been extensively characterized. Moreover, thanks to the application of a variety of Solid State Nuclear Magnetic Resonance (SSNMR) techniques, also the molecular dynamic properties of Ibuprofen in different solid forms have been characterized in detail.[15,16,17]

Especially with the aim of better modulating its fast release, which is one of the main causes of its side-effects, the possibility of incorporating Ibuprofen in Mg-Al-HTlc has been explored.[18,19,20,21,22] A positive modification of its release kinetics has been obtained[19] and, by exploiting different characterization and modelling techniques, it has been hypothesized that Ibuprofen intercalates within Mg-Al-HTlc galleries, mainly forming a monolayer in which the molecules establish a ionic interaction between their carboxylate moieties and the positively charged clay layers and orient their main axis approximately perpendicular to the layer surface. However a thorough knowledge of the status of Ibuprofen in Mg-Al-HTlc, intended as a direct and detailed characterization of its molecular dynamics properties, which are known to affect dissolution and stability properties of APIs in formulations[23,24] is still lacking.

SSNMR is an unparalleled technique for obtaining detailed and quantitative information on molecular motions, even of sub-molecular moieties, occurring over a very wide frequency range (from Hz to GHz approximately).[15,16,25,26] In this work we present a detailed charaterization of

the molecular dynamic properties of hydrotalcite-intercalated Ibuprofen, which could be obtained through a SSNMR study based on a variety of ^{1}H and ^{13}C spectral and nuclear relaxation properties, measured at variable temperature and suitably combined in a synergic analysis.

MATERIALS AND METHODS

Materials. Ibuprofen sodium salt (Na-IBU) was purchased from Sigma-Aldrich (Milan, Italy) and used in its di-hydrated form, stable at ambient conditions.[14] $AlCl_3 \cdot 6H_2O$ was obtained from Fluka (Milan, Italy) while $MgCl_2 \cdot 6H_2O$ and urea were acquired from Baker (Deventer, Holland). All the other chemicals and solvents, purchased form Sigma-Aldrich (Milan, Italy), were of reagent grade and used without further purification.

Hydrotalcite preparation. Mg-Al-HTlc, in the following indicated simply as HTlc, was prepared in carbonate form and then converted to chloride form to allow easier exchange of the intercalated anions.[27] To synthesize HTlc-CO_3, solid urea was added to an aqueous solution of $MgCl_2$ and $AlCl_3$ (0.5 M). The molar ratio of urea:(Mg+Al) and Al:(Mg+Al) were 3.3 and 0.33, respectively. Urea hydrolysis progressively increased solution pH leading to the precipitation of metals in a crystallized HTlc carbonate form.[28] The obtained solid was recovered, washed with water to eliminate chlorides, dried, and stored in a desiccator under vacuum at room temperature. Quantification of magnesium and aluminum was accomplished by ethylenediaminetetraacetic acid titration of a HTlc-CO_3 aqueous solution (50 mL) obtained by dissolving the product at pH lower than 5 with a suitable volume of HCl 0.1 N. Pure crystalline HTlc-Cl was obtained by CO_3^{2-}/Cl^- ion-exchange upon titration with a dilute HCl solution.[29]

Ibuprofen intercalation. HTlc-Cl (1.2 g) was suspended in 100 mL of Na-IBU hydroalcoholic solution (0.1 M). Briefly, Na-IBU was first solubilized in water (50 mL) and then the same volume of ethanol was poured in the aqueous solution. After adding HTlc-Cl, the suspension was maintained under magnetic stirring at 60°C for three days. The suspension was centrifuged at 4000 rpm for 5 min (Hettich Zentrifugen Universal 32R; Hettich, Tuttlingen, Germany) and washed three times with degassed water to eliminate non-intercalated IBU. The product (HTlc-IBU) was dried under vacuum and stored in a desiccator until use.

Intercalated complex characterization. Quantitative determination of Ibuprofen intercalated in the inorganic matrix was performed using ultraviolet-visible spectrophotometry (Agilent 8453 spectrophotometer; Agilent, Waldbronn, Germany). 5 mg of HTlc-IBU was solubilized in 0.5 mL HCl 6N and, after 5 minutes incubation, the solution was properly diluted with a phosphate buffer solution (pH 7.4, 0.1M) before reading the absorbance at 222 nm. The analysis was performed in triplicate and the result expressed as mean ± standard deviation. An Ibuprofen calibration curve was built in the concentration range going from 2.5 to 30 μg/mL and was characterized by a regression coefficient $r^2 > 0.999$.

Morphological evaluation of HTlc-Cl and HTlc-IBU was carried out by scanning electron microscopy (SEM) using a Field Emission SEM (LEO 1525 equipped with a GEMINI column, ZEISS, Germany). Samples were prepared by depositing the powders onto an aluminum specimen stub covered with a double sided adhesive carbon disc. Samples were sputter coated with chromium prior to imaging (Quorum Q150T ES East Grinstead, West Sussex, UK). Coating was done at 120 mA for 30 s.

Differential scanning calorimetry (DSC) was performed using a DSC 8500 calorimeter (PerkinElmer, Norwalk, USA) equipped with an intracooler (intracooler 2, PerkinElmer, Norwalk, USA). About 2 mg of sample (exactly weighted) was placed in non-hermetically sealed aluminium pans and analyzed versus an empty non-hermetically sealed aluminium pan (reference). A heating ramp from 20 to 300 °C at a scan rate of 10 °C/min was performed in inert nitrogen atmosphere.

Solid State NMR

Experiments. The NMR experiments were carried out on a Varian (Palo Alto, USA) InfinityPlus 400 spectrometer, equipped with 7.5-mm and a 3.2-mm CP-MAS probes, working at a Larmor frequency of 400.35 and 100.59 MHz for ^{1}H and ^{13}C, respectively.

The ^{1}H 90° pulse lengths were 6.0 and 2.5 μs on the 7.5 mm and 3.2 mm probes, respectively, while the ^{13}C 90° pulse length was 4.2 μs on the 7.5 mm probe. Relaxation delays of 5 s were used in all the experiments. The ^{1}H-^{13}C Cross-Polarization (CP) spectra were acquired using a contact time of 1 ms, in which the power level on the ^{13}C channel was ramped linearly to enhance CP efficiency, and the SPINAL-64 pulse sequence for ^{1}H heteronuclear decoupling. The ^{13}C direct excitation (DE) spectra were acquired using the DEPTH sequence for background suppression and continuous wave high power decoupling (HPD) from ^{1}H nuclei. In all cases a Magic Angle Spinning (MAS) frequency of 5 kHz was used. ^{13}C chemical shifts were referred to hexamethylbenzene and TMS as secondary and primary references, respectively. ^{1}H spin-lattice relaxation times in the laboratory frame (T_1) were measured using the saturation recovery pulse sequence under MAS with a spinning frequency of 5 kHz; the variable delay ranged from 5 ms to 10 s. ^{1}H T_1 at 20 and 60 °C were also measured using ^{13}C detection under ^{1}H HPD and MAS with a spinning frequency of 5 kHz. ^{13}C spin-lattice relaxation times in the laboratory frame (T_1)

were measured using the inversion recovery pulse sequence with ^{1}H HPD during ^{13}C signal acquisition, with a MAS frequency of 5 kHz; the variable delay ranged from 1 ms to 5 s. ^{13}C relaxation times were obtained by reproducing the spectra as sums of peaks through a nonlinear least-squares fit procedure using generalized Lorentzian functions as implemented in the software MNova,[30] thus allowing the integrals of each peak to be determined without the biasing effect due to peak superposition, and then the integrals vs. the variable time of the pulse sequence were fitted by means of suitable analytical functions to obtain the relaxation times.[31]

Spin-lattice relaxation times analysis. For the sake of clarity, principles of nuclear spin-lattice relaxation and the approach to the data analysis used in in this work are briefly summarized in the following.

Nuclear spin relaxation processes are determined by oscillating magnetic fields, locally generated in the sample through the modulation of the nuclear interactions operated by molecular motions. The efficiency of a relaxation mechanism, and therefore the values of the relaxation rate, defined as inverse of the corresponding relaxation time, is related to the values of the spectral densities $J(\omega)$ through equations that derive from the relaxation theory. In turn, the spectral densities can be expressed as functions of the correlation time of the molecular motion, τ_c, and of the reference frequency of the specific kind of relaxation (e.g. the Larmor frequency for spin-lattice relaxation times T_1). In particular, the trend of T_1 with temperature presents a minimum when $1/\tau_c$ of the relevant motion is of the order of the Larmor frequency, whereas T_1 decreases and increases with increasing temperature when $1/\tau_c$ is lower and higher than Larmor frequency, respectively.

For ^{13}C nuclei in natural abundance, and particularly for carbons with directly bonded protons, it is commonly assumed that the spin-lattice relaxation is dominated by dipolar interactions with

^{1}H nuclei. The relaxation time of each chemically distinct ^{13}C nucleus is influenced by the motions of the molecular rigid fragment to which the nucleus belongs. When a single motion is present, ^{13}C T_1 can be expressed as:

$$R_{1C}^{i} = \frac{1}{T_{1C}^{i}} = nK_i\left[J_i(\omega_{1H} - \omega_{13C}) + 3J_i(\omega_{13C}) + 6J_i(\omega_{1H} + \omega_{13C})\right] \quad (1)$$

where n is the number of protons directly bonded to the specific i-th carbon-13 nucleus, ω_{13C} and ω_{1H} are the Larmor frequencies of ^{13}C and ^{1}H nuclei, respectively, K_i is a measure of the effective C-H dipolar coupling experienced by the ^{13}C nucleus, which at most can assume the value of the static C-H dipolar coupling, K_s:

$$K_s = \frac{1}{20}\left(\frac{\mu_0}{4\pi}\frac{\gamma_H\gamma_C\hbar}{r_{CH}^{3}}\right)^2 \quad (2)$$

with μ_0 the magnetic vacuum permeability, r_{CH} the C-H bond distance, γ_H and γ_C the gyromagnetic ratios for ^{1}H and ^{13}C, respectively. K_i can be less than K_s in the presence of fast motions reducing the effective dipolar interaction with respect to its theoretical value.[32,33,34]

When different motions are considered to affect a relaxation curve, if they are assumed independent, as it will be done here, their contributions to the relaxation rate can be considered as additive:

$$R_{1C,Tot}^{i} = \sum_{j} R_{1C,j}^{i} \quad (3)$$

where $R^{i}_{1C,j}$ is the contribution to the relaxation rate of the i-th ^{13}C nucleus due to the j-th motion, expressed by eq. 1.

As far as ^{1}H T_1 relaxation is concerned, the spin diffusion phenomenon, which is negligible for rare ^{13}C nuclei, has to be taken into account. In this work, a single average relaxation rate

($<1/T_1>$) was measured, which contains the contributions of all the motions affecting the spin-lattice relaxation of all the protons in the sample.

In this case, the relationship linking $<1/T_1>$ to the spectral densities is:

$$\left\langle \frac{1}{T_1} \right\rangle = C \sum_l a_l \left[J_l(\omega_{1H}) + 4J_l(2\omega_{1H}) \right] \qquad (4)$$

where ω_{1H} is the proton Larmor frequency, C is a constant related to the fraction of second moment corresponding to the dipolar interaction available for the relaxation process and the sums run over the number of motional processes, each contributing to the relaxation with the relative weight a_l.

To express the spectral densities $J(\omega)$ in terms of the correlation time of the motion τ_C the simplest model devised by Bloembergen-Purcell-Pound (commonly referred to as BPP) was used. Within this model, the analytical expression for the spectral densities is the following:

$$J^{BPP}(\omega) = \frac{2\tau_C}{1+\omega^2\tau_C^2} \qquad (5)$$

For describing the dependence of τ_C on temperature the Arrhenius law was used:

$$\tau_C = \tau_\infty \exp\left(\frac{E_a}{kT}\right) \qquad (6)$$

where τ_∞ is the correlation time in the limit of infinite temperature and E_a is the activation energy of the motion.

RESULTS AND DISCUSSION

Preparation and characterization of the intercalated complex. With the aim of obtaining an intercalated complex of Ibuprofen (IBU), an Mg-Al hydrotalcite (HTlc) matrix was first prepared in carbonate form and then converted to chloride form[35] (HTlc-Cl) to facilitate the ion exchange process.[36] In fact, it known that the CO_3^{2-} anions are strongly held in the interlayer region and that it is difficult to exchange them with other anions using simple ion exchange procedures. Cl^- anions can be replaced more easily than carbonates because they are monovalent anions, the interactions of which with the lamellae are weaker.[36] The composition of HTlc-Cl was the following: $Mg_{0.62}Al_{0.38}(OH)_2.Cl_{0.38} \cdot 0.56\ H_2O$. The intercalation product (HTlc-IBU) obtained from HTlc-Cl and Ibuprofen Sodium salt (Na-IBU), was analyzed by UV-vis spectrophotometry and the Ibuprofen content was found to be 52.7 ± 1.6 % (w/w), consistent with the literature data.[37] Photomicrographs of HTlc-Cl (a, b) and HTlc-IBU (c, d) show regular flattened crystals with diameter around 3 μm that appear as circles piled up one on the other. Besides, the intercalation process did not affect the morphology or dimensions of the particles (Figure 1).

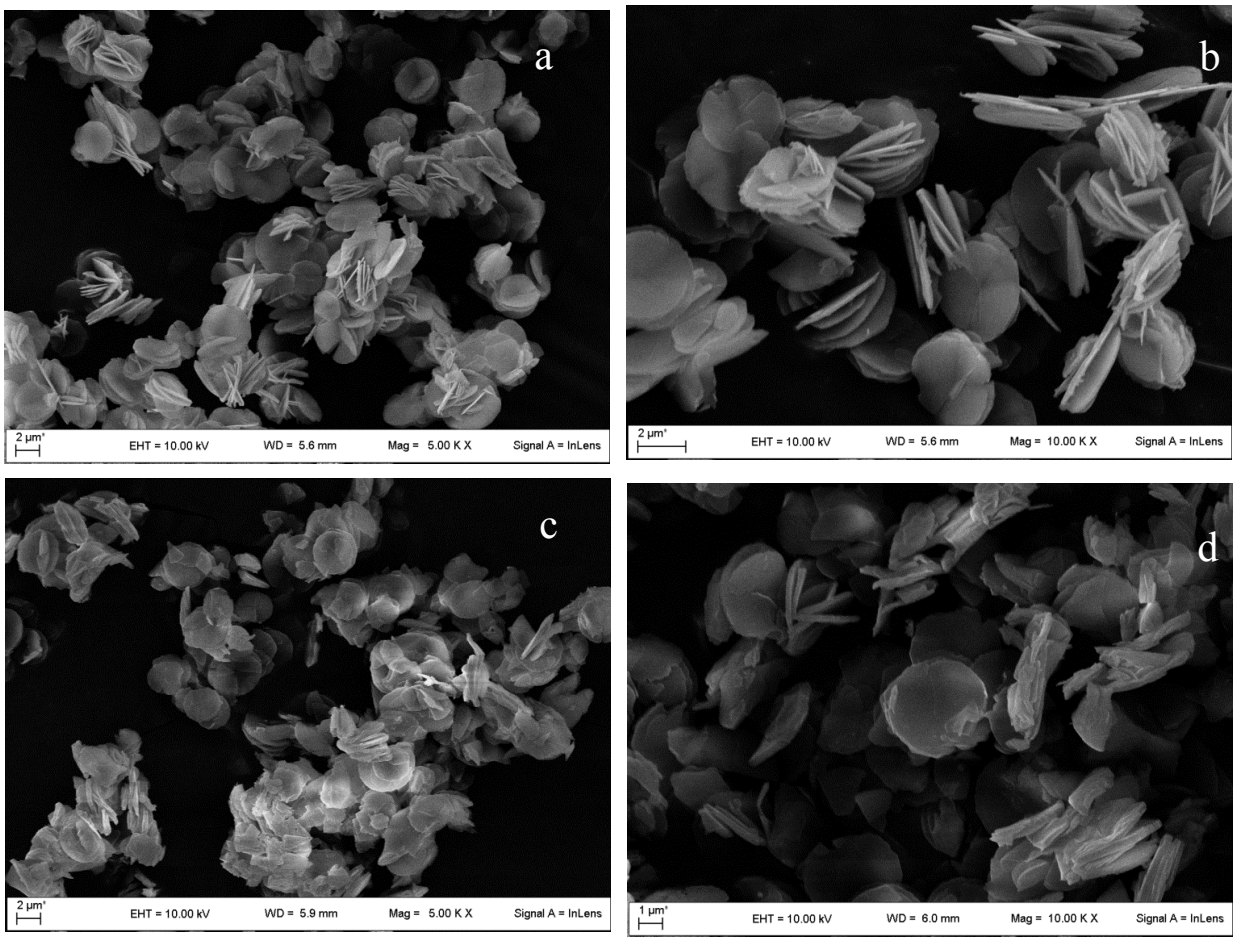

Figure 1. Photomicrographs of HTlc-Cl (a, b) and HTlc-IBU (c, d) at different magnifications.

In Figure 2 DSC thermograms recorded on Na-IBU, HTlc-Cl and HTlc-IBU are reported. DSC data show two endothermic events for pure Na-IBU: the first event at ~ 75 °C is ascribable to crystal dehydration, while the second sharper endothermic event at ~ 200 °C (199.3 ± 1.5 °C) corresponds to the melting of anhydrous sodium ibuprofen.[38,39] When HTlc-Cl was submitted to the same temperature ramp, the sole detectable event was a very broad endothermic event with a maximum at 105 ± 4 °C, ascribable to the vaporization of the water molecules contained in the structure. In the DSC thermogram of HTlc-IBU the characteristic endothermic events of IBU and HTlc are no more visible, indirectly confirming the intercalation of Ibuprofen in the HTlc matrix. In particular, the absence of the endothermic peak at ~ 200 °C (due to the melting of anhydrous

sodium ibuprofen) excludes the presence of crystalline Ibuprofen and corroborates the occurred intercalation.

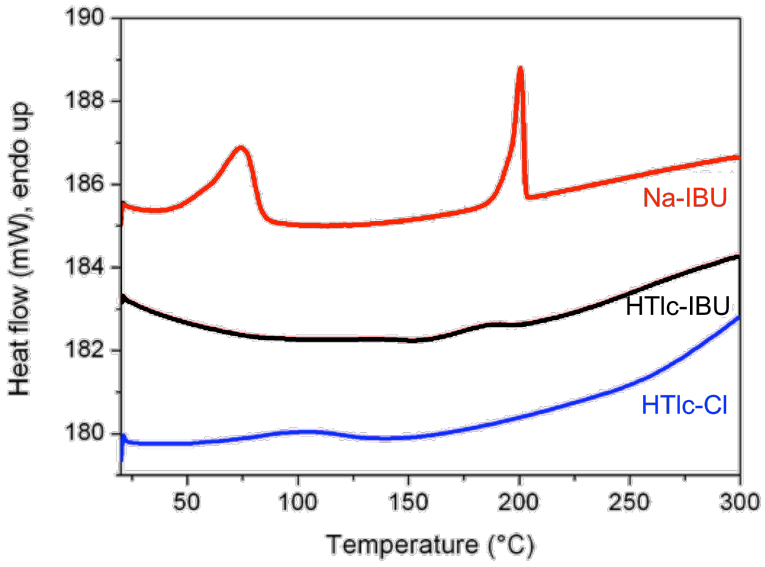

Figure 2. DSC thermograms of Na-IBU, HTlc-Cl, and HTlc-IBU.

^{1}H and ^{13}C MAS NMR spectra. High-resolution ^{1}H and ^{13}C MAS NMR spectra were recorded on the investigated samples. In general, very high MAS frequencies are required to averaged out the ^{1}H homonuclear dipolar coupling and obtain a good resolution in ^{1}H spectra; however, the obtained resolution is also dependent on the averaging of the coupling performed by molecular motions. In Figure 3 the ^{1}H MAS spectra of HTlc-Cl and HTlc-IBU, recorded at a spinning speed of 20 kHz, are reported and compared with the ^{1}H MAS spectrum of Na-IBU.[40] The spectrum of HTlc-Cl is constituted by two broad signals: one very intense at about 5 ppm and another, much weaker, at about 7.5 ppm. The first signal is ascribable to protons of water molecules and hydroxyl groups of hydrotalcite. This is in agreement with previously reported ^{1}H

MAS spectra, which, at spinning frequencies higher than 30 kHz, show two separated signals resonating at 4.8 ppm and 3.8 ppm, assigned to protons of water molecules and Mg_2Al-OH, respectively.[41] The weaker, broad signal at about 7.5 ppm can arise from a fraction of protons, either of water or Mg_2Al-OH, subjected to quite strong H-bonds. The presence of water molecules within HTlc-Cl has been detected also by DSC experiments. In the spectrum of Na-IBU two signals are resolved, which are ascribed to aliphatic (1.0 ppm) and aromatic (7.0 ppm) protons. Comparing the spectrum of HTlc-IBU with those of pristine HTlc-Cl and Na-IBU it can be noticed that the signals of HTlc-Cl remain substantially unchanged (although the broad signal at 7.5 ppm cannot be clearly resolved in the spectrum of HTlc-IBU), while those of Ibuprofen (IBU) look very different with respect to those in the spectrum of Na-IBU. Indeed, even if there are not significant changes in the chemical shift values, the linewidth of all the signals is significantly reduced, so that three different peaks are clearly resolved in the aliphatic region at about 1.0, 2.4 and 3.7 ppm, not distinguishable in the spectrum of Na-IBU. In particular the average value of the width at half height changes from 1100 Hz in Na-IBU to 300 Hz in HTlc-IBU. Although a direct interpretation of the linewidths is not straightforward, because of the partial average operated by MAS, their significant reduction observed in passing from Na-IBU to HTlc-IBU (in the same MAS conditions) indicates the presence of a larger molecular mobility, able to strongly reduce the average proton-proton homonuclear dipolar interactions.

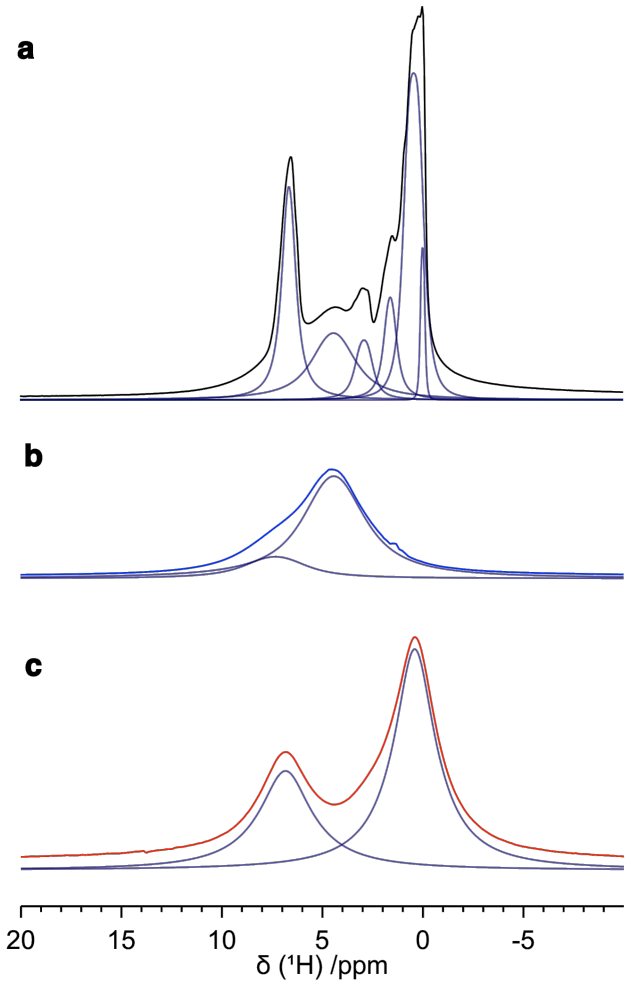

Figure 3. ^{1}H MAS spectra of HTlc-IBU (a), HTlc-Cl (b), and Na-IBU (c), recorded with a spinning frequency of 20 kHz. Peaks obtained from spectral deconvolution are reported in blue.

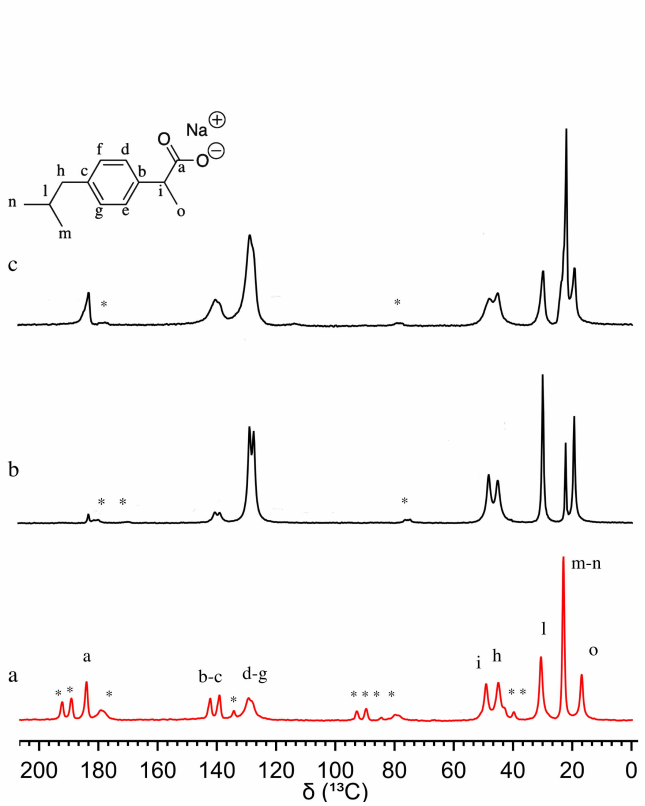

Figure 4. ^{13}C CP-MAS spectra of Na-IBU[40] (a) and HTlc-IBU (b), and ^{13}C DE-MAS spectrum of HTlc-IBU (c). Spinning sidebands are marked with asterisks. In the inset the chemical formula of Na-IBU is reported with carbon labelling used in the text.

The ^{13}C MAS spectra of Na-IBU and HTlc-IBU are reported in Figure 4. The ^{13}C CP-MAS spectrum of HTlc-IBU presents significant differences with respect to that of Na-IBU (Figure 4a,b and Table 1).[40] First it can be noticed that the signals of carbons **a**, **b**, **i** and **o** are all shifted with respect to those of Na-IBU. These carbons belong to the isopropionic fragment, with the exception of **b**, which is the quaternary aromatic carbon directly bonded to it: therefore, the isopropionic fragment experiences a remarkable change in its chemical environment after intercalation. This indication strongly supports the formation of an interaction between IBU and hydrotalcite layers involving the carboxylate group. Such interaction was previously hypothesised in the literature on the basis of FT-IR data.[19] Moreover, the shift of the signal of carbon **o**, resonating at 19.7 ppm in HTlc-IBU, 2.5 ppm more than in Na-IBU, was reported to be

diagnostic of the full intercalation of IBU molecules,[42,43] which is therefore here experimentally verified. Secondly, the signals of ternary aromatic carbons (**d-g**) significantly change their shape and intensity, becoming narrower and more intense in passing from Na-IBU to HTlc-IBU. This suggests a modification of the ring dynamics when IBU is intercalated in HTlc. Finally, the signal of carbons **m** and **n** has a significantly reduced intensity in the spectrum of HTlc-IBU with respect to that of Na-IBU, which can be caused by a different dynamics of the two methyl groups in the two samples. In order to investigate this aspect, ^{13}C DE-MAS experiments were performed on HTlc-IBU (Figure 4c). From the comparison between CP and DE spectra we can see that the reduced intensity of the signal of **m** and **n** is peculiar of the CP spectrum, thus indicating that the polarization transfer from protons is less efficient for these two methyl carbons in HTlc-IBU than in Na-IBU. The minor efficiency of the polarization transfer is probably due to the reduction of the effective dipolar coupling between carbon and proton nuclei, in turn due to a larger mobility affecting these molecular groups in HTlc-IBU. In addition, it can be noticed that in the CP spectrum of HTlc-IBU the spinning sidebands of carboxylic (**a**) and aromatic carbons (**b-g**) are present in a smaller number and with a reduced intensity with respect to the spectrum of Na-IBU recorded at the same spinning frequency. This can be straightforwardly ascribed to a reduced chemical shift anisotropy (CSA), in turn ascribable to an increased mobility of part or of the whole IBU molecules in the intercalated compound.

Table 1. ^{13}C chemical shift values of the signals in CP-MAS spectra of Na-IBU[40] and HTlc-IBU (Figure 4). Carbon labels are defined in Figure 4.

	^{13}C Chemical shift (ppm)	
^{13}C Nuclei	Na-IBU	HTlc-IBU
a	184.2	183.5
b	142.5	140.8
c	139.4	139.1
d-g	126-133	127.7,129.2
h	45.3	45.4
i	49.4	48.6
l	31.0	30.2
m-n	23.4	22.7
o	17.2	19.7

In order to further investigate the dynamic properties of intercalated IBU, ^{13}C CP-MAS and DE-MAS spectra of HTlc-IBU were recorded in the temperature range 20 - 60 °C (Figure 5). In both the series of spectra no dramatic changes are observed, indicating that no phase transitions or chemical transformations occur in this temperature interval. It is worth noticing that in the spectra of HTlc-IBU two well separated peaks can be observed for the ternary aromatic carbons (**d-g**) at all temperatures, while in Na-IBU at room temperature they gave rise to two heavily superimposed signals appearing as almost a single broad peak, which transformed into two separated peaks at higher temperatures.[16] The room temperature broadening observed for Na-

IBU was ascribed to the interference between the motional frequency of the π-flip of the aromatic ring and either the MAS or HPD frequency (both in the range of kHz).[44,45] The present observation suggests that, while in Na-IBU the frequency of the π-flip of the aromatic ring at room temperature is in the kHz regime, it is higher in HTlc-IBU. Also the signal of carbons **m** and **n** does not change significantly in the temperature range investigated, and therefore also for the isobutyl group the frequency of the motion is too high to affect the lineshape of the corresponding signal, as already observed in the case of Na-IBU.[16]

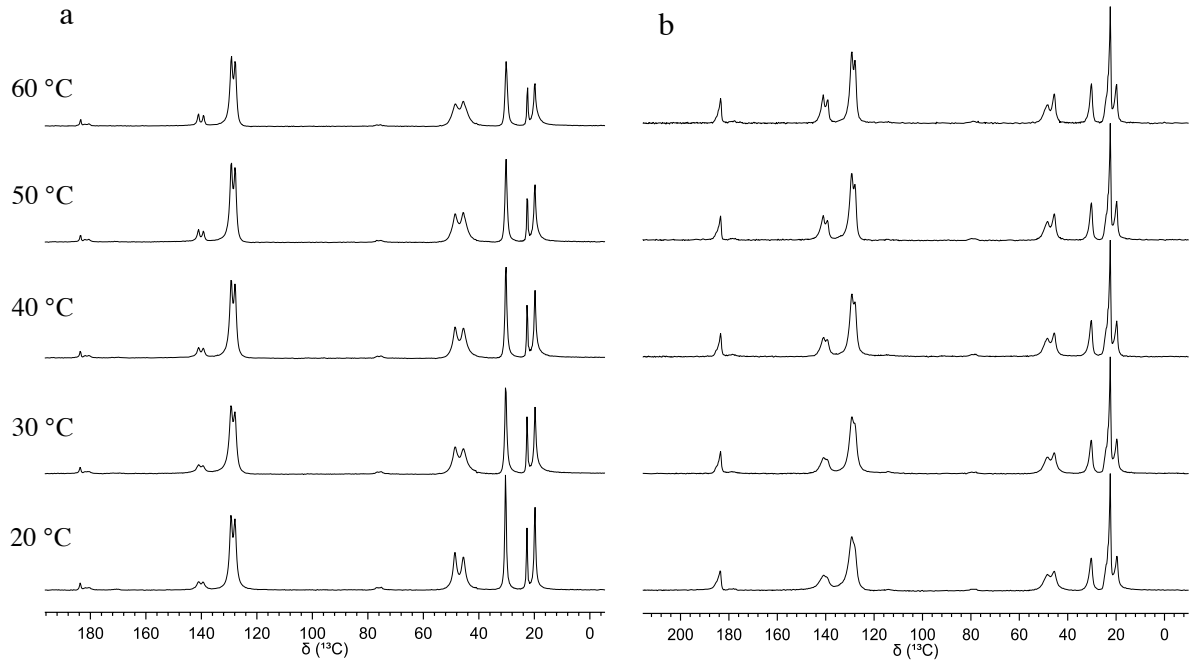

Figure 5. ^{13}C CP-MAS (a) and DE-MAS (b) spectra of HTlc-IBU recorded at the indicated temperatures.

^{13}C T_1 relaxation times. ^{13}C spin lattice relaxation times (T_1) were measured for each carbon nucleus of IBU in HTlc-IBU: these values are reported, along with those of Na-IBU, available from a previous work,[16] in Table 2. Noticeable differences between the values obtained for HTlc-IBU and Na-IBU are clearly observed. For Na-IBU only the carbon nuclei of methyl (**m**, **n**, **o**)

and isobutyl (**h**, **l**) groups were previously found to have T_1 values below 1 s, due to the occurrence of fast motions of the fragments which these carbons belong to (methyl rotations about their ternary symmetry axes and intercoformational motion of the isobutyl group). Instead, the remaining carbon nuclei of Na-IBU showed much longer T_1 values, indicating that neither overall molecular motions nor reorientational motions of the phenyl and the isopropionic groups occurred in the MHz regime. On the other hand, in HTlc-IBU methyl and isobutyl carbons show T_1 values of the same order of magnitude than in Na-IBU, while all the other carbons have T_1 values about one order of magnitude shorter with respect to Na-IBU. In particular, all T_1 values range between 0.3 and 0.9 s, with the exception of quaternary carbons, showing T_1's of 1.6-2.0 s. This strongly suggests that, contrary to what happens in Na-IBU, the ^{13}C spin-lattice relaxation in HTlc-IBU is heavily affected by a motion involving the whole molecule.

Table 2. ^{13}C T_1 values measured for IBU[16] and HTlc-IBU. Carbon labels are defined in Figure 4.

	T_1 (s)	
^{13}C nucleus	IBU	HTlc -IBU
a	46 ± 2	1.6 ± 0.5
b	20 ± 2	2.0 ± 0.5
c	9 ± 1	2.0 ± 0.5
d-g	5 ± 0.5	0.42 ± 0.05
h	0.44 ± 0.05	0.40 ± 0.1
i	10.9 ± 0.2	0.86 ± 0.1
l	0.86 ± 0.02	0.61 ± 0.05
m-n	0.40 ± 0.01	0.51 ± 0.01
o	0.15 ± 0.01	0.35 ± 0.05

Variable temperature ^{1}H and ^{13}C T_1 relaxation times. ^{1}H T_1's were measured in the temperature range 20-60 °C for the sample HTlc-IBU. A single ^{1}H T_1 value was found at all temperatures, indicating that, as expected, the average of T_1's of different ^{1}H nuclei, operated by spin diffusion, was complete. However, in order to separate the contribution to the relaxation arising from IBU and HTlc protons, the relaxation times were measured *via* both direct observation of ^{1}H nuclei and ^{13}C detection. The first experiment reveals contributions to relaxation of all the ^{1}H nuclei in the sample, while only ^{1}H nuclei dipolar coupled to ^{13}C nuclei (thus belonging to IBU only) contribute to the second experiment. Since the two experiments gave very similar T_1 values, the contribution of the protons of HTlc to ^{1}H spin-lattice relaxation could be safely neglected. The measured ^{1}H T_1 values range from 0.47 to 0.45 s with a quite flat trend with temperature (Figure 6i). Due to its average nature, T_1 values are in principle determined by all the motions occurring throughout the sample and therefore a simple interpretation of the curve of ^{1}H T_1 *vs* temperature alone is not possible. However, this curve was used to validate the model devised on the basis of ^{13}C T_1's analysis (*vide infra*).

Variable temperature ^{13}C T_1's were measured for all the carbon nuclei and were analysed in order to characterize the molecular motions involved in the relaxation mechanisms. The trends of ^{13}C T_1's with temperature are shown in Figure 6 (a-h): while T_1's of carbons **o** and **m**/**n** increase with temperature, the values for all the other carbons slightly decrease with temperature. This could be explained with the previously hypothesized occurrence of an overall molecular motion affecting all carbon nuclei, with the addition, for methyl carbons only, of the ubiquitous fast rotation of methyl groups around their three-fold symmetry axis, which causes the increasing trend of the T_1's of carbons **o** and **m**/**n** with temperature.

In order to verify this hypothesis, a quantitative and simultaneous analysis of all the relaxation times *vs* temperature curves was performed. A precise model that takes into account all the potential molecular motions is not straightforward and some assumptions have to be made. In particular we followed the criterion of using the smallest number of molecular motions able to reproduce the experimental data with physical meaningful parameters and, when possible, we used information from independent experiments to support the model. First a motion involving the whole molecule was considered since all the experimental data suggested its presence; this motion is expected to affect the relaxation of all the ^{13}C nuclei of IBU. Moreover, some internal interconformational motions had to be considered because, on one hand, they were necessary to reproduce T_1's experimental values and, on the other hand, were also found to substantially contribute to similar T_1 values measured in the case of Na-IBU.[16] In particular, the following motions were taken into account: (i) an overall molecular motion, which influences T_1's of all the carbons; (ii) the rotation of the methyl groups around their three-fold symmetry axes, affecting T_1's of methyl carbons only; (iii) the interconformational motion of the isobutyl group, affecting T_1's of carbons **h**, **l**, **m** and **n**; (iv) the rotation of the aromatic ring about its para-axis, affecting T_1 relaxation of carbons **d-g**.

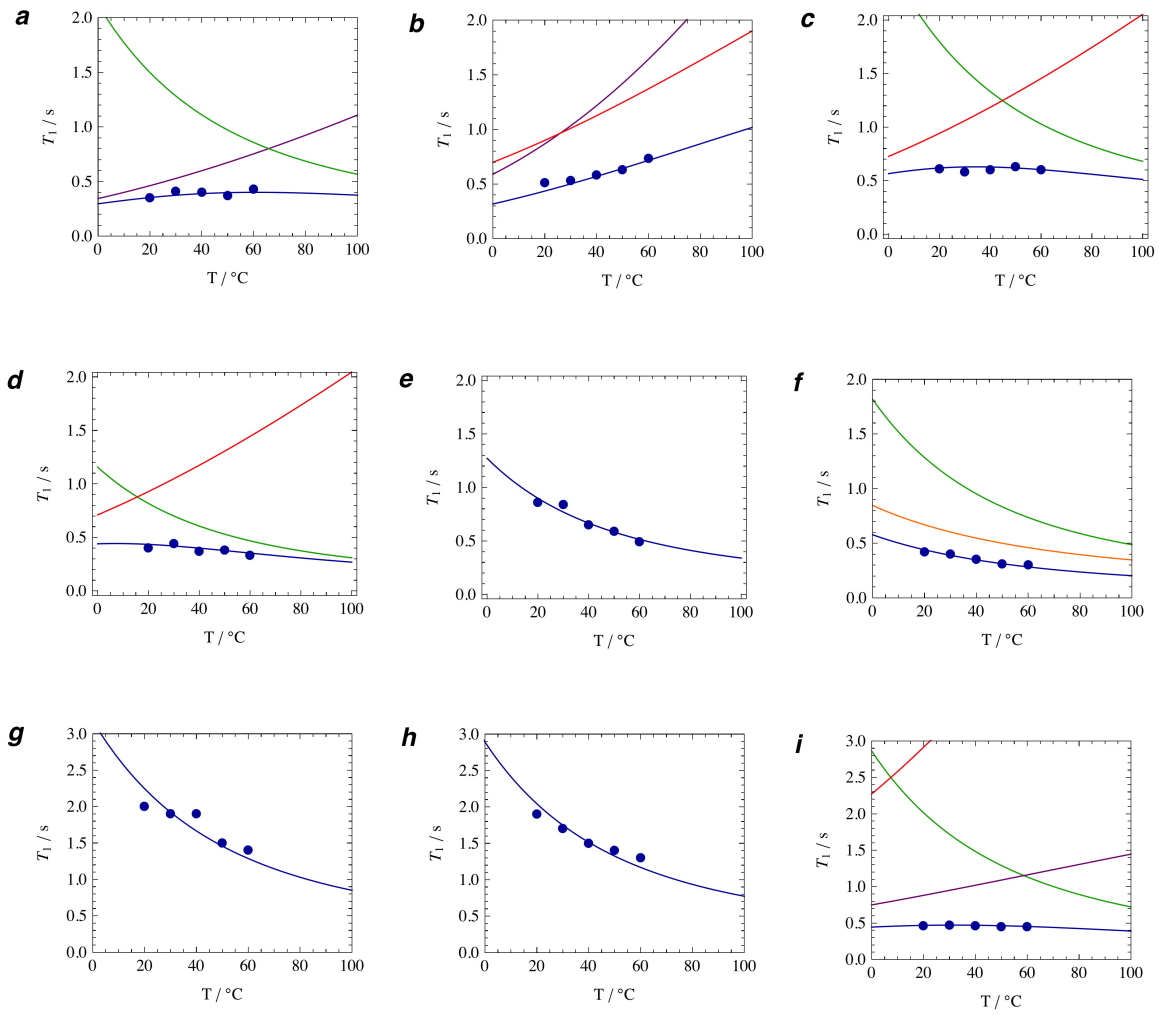

Figure 6. (a-h) Curves of ^{13}C spin-lattice relaxation times (T_1) *vs.* temperature measured at a Larmor frequency of 100.56 MHz for HTlc-IBU: (a) carbon **o**, (b) carbons **m** / **n** (signal at 23 ppm), (c) carbon **l**, (d) carbon **h**, (e) carbon **i**, (f) carbons **d**-**g**, (g) carbons **b** / **c**, and (h) carbon **a**. (i) Curve ^{1}H T_1 *vs.* temperature measured at a Larmor frequency of 400.35 MHz. Symbols and blue lines indicate experimental and calculated relaxation times, respectively. Purple, green, red, and orange lines in (a)-(d), (f) and (i) indicate the contribution of methyl rotations, those of the motion of the whole molecule, that of the isobutyl motion, and that of the aromatic ring motion, respectively.

The analysis was carried out by means of a global fitting procedure, consisting in the simultaneous fitting of the curves T_1 vs. temperature of all protonated carbons through the equations 1-3, 5, 6 (see "Spin-lattice relaxation times analysis" in Materials and Methods section). The fitting curves are shown in Figures 6 a-f. The motional parameters (activation

energies and correlation times) were determined as best-fitting parameters and are reported in Table 3. Moreover, the curves T_1 vs. temperature of the quaternary ^{13}C nuclei and of the ^{1}H nuclei were simulated using equations 1-6 and the motional parameters obtained by the fitting (Figure 6 g-i). In all cases the agreement between the best-fitting curves and the experimental trend is very good.

All the multiplying factors a_l of Eq. 4 obtained from the fitting procedures are smaller than or equal to 1, as expected. It is worth noticing that the experimental data could be well reproduced even without considering the motion (iv), i.e. the reorientation of the aromatic ring about its para axis. However, such fit gave as a result a K_i value (see Eq. 1) of $1.9 \cdot K_s$ for the ternary aromatic carbons (**d**-**g**), which is physically unreasonable, as discussed above. Indeed, the introduction of the motion (iv), which has a similar effect than the overall molecular motion on the relaxation of ternary aromatic carbons, substantially resulted in giving physically meaningful values of $K_i \approx K_s$ for both motions (i) and (iv). Although the assumption of considering these two motions as independent is quite rough (also because they result to have correlation times of the same order of magnitude – about 10^{-8} s at room temperature), the presence of both these motions seem fully reasonable, also considering that motion (iv) is active and shows a similar correlation time even in pristine Na-IBU.[16]

Table 3. Motional parameters for HTlc-IBU obtained from the fit of experimental data as described in the text. E_a and τ_∞ were obtained from the fitting procedure, and they were used to calculate τ_C at temperature equal to 25 °C, through the Arrhenius equation (Eq. 6). τ_C values calculated at 25 °C of Na-IBU, taken from ref.16, are also reported for comparison.

	HTlc-IBU			Na-IBU
Motion	E_a (kJ/mol)	Log(τ_∞ (s))	τ_C (s) @ 25 °C	τ_C (s) @ 25 °C
Motion of the whole molecule	12	-9.9	$1.5\ 10^{-8}$	-
Methyl **o** rotation	10	-12.3	$3.2\ 10^{-11}$	$3.5\ 10^{-11}$
Methyls **m**/**n** rotation	13	-12.8	$3.0\ 10^{-11}$	$2.1\ 10^{-11}$
Isobutyl reorientation	9	-11.9	$4.8\ 10^{-11}$	$3.9\ 10^{-10}$
Aromatic ring motion	8	-9.4	$1.1\ 10^{-8}$	$9.1\ 10^{-7}$

The comparison between the ^{1}H MAS (Figure 3) and ^{13}C MAS (Figure 4) spectra of Na-IBU and HTlc-IBU suggests that in the latter sample IBU should span, because of the overall molecular motion, a wider range of orientations with respect to that associated with the spinning of the molecule about its "long molecular axis" (Figure 7). Indeed in Na-IBU the π-flip of the aromatic ring and the interconformational motion of the isobutyl group, which, together, can be considered similar to the overall rotation of the molecule about its long axis, are not able to produce the same line-narrowing observed in the ^{1}H MAS spectrum of IBU-HTlc. Moreover, the the π-flip of the aromatic ring results in Na-IBU in a much larger ^{13}C chemical shift anisotropy than that observed in IBU-HTlc. Therefore, in IBU-HTlc a motion with a different geometry must be present, able to cause a much stronger reduction of the proton homonuclear dipolar

coupling and of the carbon chemical shift anisotropy, which should permit the whole IBU molecule to span a much wider range of orientations than in Na-IBU. Considering that the carboxylate anion interacts with HTlc layer through an ionic bond, it is plausible that IBU in HTlc experiences a *wobbling in a cone* motion[46,47,48] (Figure 7), which is also compatible with all the other experimental results.

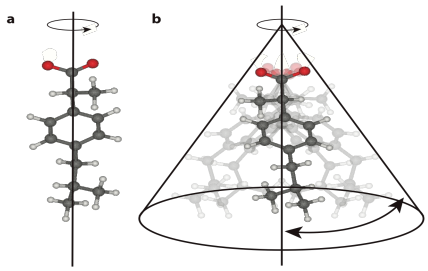

Figure 7. Schematic representation of a spinning (a) and wobbling-in-a-cone (b) motion of IBU.

CONCLUSIONS

The global analysis of a variety of spectral and relaxation SSNMR experiments provided a detailed characterization of the molecular dynamics properties of Ibuprofen intercalated in Mg-Al-hydrotalcite, which resulted to be very different with respect to those of pristine sodium Ibuprofen in its thermodynamically stable crystalline form.

The strong reduction of the ^{1}H MAS line-width observed in HTlc-IBU with respect to Na-IBU indicated that the proton homonuclear dipolar couplings are largely averaged out by molecular motions in HTlc-IBU, which implies the presence of a motion involving all (or almost all) the

protons of IBU. The reduction of the chemical shift anisotropy of the aromatic carbons, observed by the smaller number and reduced intensity of spinning sidebands in ^{13}C MAS spectra of HTlc-IBU, suggested the presence of a motion involving the phenyl ring with a different geometry with respect to the π-flip motion already present in Na-IBU. Both these observations concurred in indicating the presence in HTlc-IBU of a molecular motion with a motional frequency larger than the static linewidths (of the order of tens of kHz), able to span many more molecular orientations than a rotation of the IBU molecule about its long molecular axis. Also on the basis of ^{13}C T_1 relaxation times, a plausible model for this motion could be the *wobbling-in-a-cone*, with IBU being "anchored" to the hydrotalcite surface through the carboxylate moiety. Moreover, the analysis of ^{13}C and ^{1}H T_1's measured at variable temperature allowed us to recognize and quantitatively characterize in terms of activation energies and correlation times the fast rotations of all the methyl groups about their three-fold symmetry axes, of the isobutyl group and of the aromatic ring about its para axis, the last two motions resulting faster than in Na-IBU.

This study represents an example of how a detailed characterization of the motions involving organic molecules in complex systems can be performed through the combined use of several NMR observables, exploiting both different nuclei (^{1}H and ^{13}C) and different nuclear properties (spectral properties and relaxation times).

The results obtained represent the first detailed dynamic characterization of Ibuprofen intercalated in Mg-Al-hydrotalcite, which allows a complete picture of the status of this important API intercalated in an interesting carrier as hydrotalcite to be drawn. This can open the way to an improved understanding and optimization of the release properties of this and similar formulations.

AUTHOR INFORMATION

Corresponding Authors

* Marco Geppi, Dipartimento di Chimica e Chimica Industriale, Università di Pisa, via G. Moruzzi 13, 56124, Pisa, Italy. Phone: +39-0502219289; e-mail:marco.geppi@unipi.it

* Elisa Carignani, Dipartimento di Chimica e Chimica Industriale, Università di Pisa, via G. Moruzzi 13, 56124, Pisa, Italy. Phone: +39-0502219353; e-mail:elisa.carignani@for.unipi.it

Author Contributions

The manuscript was written through contributions of all authors. All authors have given approval to the final version of the manuscript.

ACKNOWLEDGMENT

The authors would like to acknowledge the contribution of the COST Action CA15209 (Eurelax: European Network on NMR Relaxometry); E.C. thanks the PhD School "G. Galilei", University of Pisa, for a fellowship.

REFERENCES

[1] Van den Mooter, G. The use of amorphous solid dispersions: A formulation strategy to overcome poor solubility and dissolution rate. *Drug Discov. Today Technol.* **2012**, *9*, e79-e85.

[2] Maleki, A.; Kettiger, H.; Schoubben, A.; Rosenholm, J. M.; Ambrogi, V.; Hamidi, M. Mesoporous silica materials: From physico-chemical properties to enhanced dissolution of poorly water-soluble drugs. *J. Control. Release* **2017**, *262*, 329-347.

[3] Perioli, L.; Pagano. C. Inorganic matrices: an answer to low drug solubility problem. *Expert Opin. Drug Deliv.* **2012**, *9*, 1559-1572.

[4] Konturek, J.W.; Beneke, M.; Koppermann, R.; Petersen-Braun, M.; Weingärtner, U. The efficacy of hydrotalcite compared with OTC famotidine in the on-demand treatment of gastroesophageal reflux disease: a non-inferiority trial. *Med. Sci. Monit.* **2007**, *13*, CR44-49.

[5] Scholtz, E.C.; Feldkamp, J.R.; White, J.L.; Hem, S.L. Properties of carbonate-containing aluminum hydroxide produced by precipitation at constant pH, *J. Pharm. Sci.* **1984**, 73, 967-973.

[6] Rives, V.; del Arco, M.; Martín, C. Intercalation of drugs in layered double hydroxides and their controlled release: A review. *Appl. Clay Sci.* **2014**, *88-89*, 239-269.

[7] Rives, V.; del Arco, M.; Martín, C. Layered double hydroxides as drug carriers and for controlled release of non-steroidal antiinflammatory drugs (NSAIDs): A review. *J. Control. Release* **2013**, *169*, 28-39.

[8] Mishra, G.; Barsha Dash, B.; Pandey S. Layered double hydroxides: A brief review from fundamentals to application as evolving biomaterials. *Appl. Clay Sci.* **2018**, *153*, 172-186.

[9] Parello, M. L.; Rojas, R.; Giacomelli, C. E. Dissolution kinetics and mechanism of Mg–Al layered double hydroxides: A simple approach to describe drug release in acid media. *J. Colloid Interface Sci.* **2010**, *351*, 134-139.

[10] Xu, F.; Sun, L. X.; Tan, Z. C.; Liang, J. G.; Li, R. L. Thermodynamic study of ibuprofen by adiabatic calorimetry and thermal analysis. *Thermochim. Acta* **2004**, *412*, 33-37.

[11] Goossens, D. J.; Heerdegen, A. P.; Welberry, T. R.; Beasley, A. G. The molecular conformation of Ibuprofen, $C_{13}H_{18}O_2$, through X-ray diffuse scattering. *Int. J. Pharm.* **2007**, *343*, 59-68.

[12] Brás, A. R.; Noronha, J. P.; Antunes, A. M. M.; Cardoso, M. M.; Schönhals, A.; Affouard, F.; Dionísio, M.; Correia, N. T. Molecular motions in amorphous ibuprofen as studied by broadband dielectric spectroscopy. *J. Phys. Chem. B* **2008**, *112*, 11087-11099.

[13] Zhang, G. G. Z.; Paspal, S. Y. L.; Suryanarayanan, R.; Grant, D. J. W. Racemic species of sodium ibuprofen: characterization and polymorphic relationships. *J. Pharm. Sci.* **2003**, *92*, 1356-1366.

[14] Rossi, P.; Macedi, E.; Paoli, P.; Bernazzani, L.; Carignani, E.; Borsacchi, S.; Geppi, M. Solid-solid transition between hydrated racemic compound and anhydrous conglomerate in na-ibuprofen: A combined X-ray diffraction, solid-state NMR, calorimetric, and computational study. *Cryst. Growth Des.* **2014**, *14*, 2441-2452.

[15] Carignani, E.; Borsacchi, S; Geppi, M. Detailed characterization of the dynamics of ibuprofen in the solid state by a multi-technique NMR approach. *ChemPhysChem* **2011**, *12*, 974 – 981.

[16] Carignani, E.; Borsacchi, S.; Geppi, M. Dynamics by Solid-State NMR: Detailed study of ibuprofen na salt and comparison with ibuprofen. *J. Phys. Chem. A* **115**, 8783–8790 (2011).

[17] Concistrè, M.; Carignani, E.; Borsacchi, S.; Johannessen, O. G.; Mennucci, B.; Yang, Y.; Geppi, M.; Levitt, M. H. Freezing of molecular motions probed by cryogenic magic angle spinning NMR. *J. Phys. Chem. Lett.* **2014**, *5*, 512.

[18] Mohanambe, L.; Vasudevan, S. Anionic clays containing anti-inflammatory drug molecules: comparison of molecular dynamics simulation and measurements. *J. Phys. Chem. B* **2005,** *109,* 15651-15658.

[19] Ambrogi, V.; Fardella, G.; Grandolini, G.; Perioli, L. Intercalation compounds of hydrotalcite-like anionic clays with antiinflammatory agents - I. Intercalation and in vitro release of ibuprofen. *Int. J Pharm.* **2001**, *220*, 23–32.

[20] Costantino, U.; Ambrogi, V.; Nocchetti, M.; Perioli, L. Hydrotalcite-like compounds: Versatile layered hosts of molecular anions with biological activity *Micropor. Mesopor. Mat.* **2008**, *107*, 149–160.

[21] Sousa, R.; Jenny Jouin, J.; Olivier Masson, O.; Fabien Remondiere, F.; Alex Lemarchand, A.; Maggy Colas, M.; Philippe Thomas, P.; Jerônimo Lameira, J.; Bastos, G. N. T.; Lima, A. B.; Nascimento, J. L. M.; Marcos Anicete□Santos, M.; Monteiro, W. R.; Alves, C. N. Structure and analgesic properties of layered double hydroxides intercalated with low amounts of ibuprofen. *J Am. Ceram. Soc*. **2017**, *100*, 2712-2721.

[22] Conterosito, E.; Van Beek, W.; Palin, L.; Croce, G.; Perioli, L.; Viterbo, D.; Gatti, G.; Milanesio, M. Development of a fast and clean intercalation method for organic molecules into layered double hydroxides. *Cryst. Growth Des.* **2013**, *13*, 1162-1169.

[23] Byrn, S. R.; Xu, W.; Newman, A. W.; Chemical reactivity in solid-state pharmaceuticals: formulation implications. *Adv. Drug Deliver. Rev.* **2001**, *48*, 115-136.

[24] Yoshioka, S.; Aso, Y. Correlations between molecular mobility and chemical stability during storage of amorphous pharmaceuticals. *J. Pharm. Sci.* **2007**, *96*, 960-981.

[25] Geppi, M.; Mollica, G.; Borsacchi, S.; Veracini, C.A. Solid-State NMR Studies of Pharmaceutical Systems. *Appl. Spectrosc. Rev.* **2008**, *43*, 202-302.

[26] Geppi, M.; Borsacchi, S.; Carignani, E. Study of Disorder by Solid-State NMR Spectroscopy. In *Disordered Pharmaceutical Materials*, 1st ed.; Descamps, M. Ed.; Wiley-VCH: Weinheim, 2016; pp. 427-466.

[27] Schoubben, A.; Blasi, P.; Giovagnoli, S.; Rocchetti, M.; Ricci, M.; Perioli, L.; Rossi, C. Evaluation and optimization of the conditions for an improved ferulic acid intercalation into a synthetic lamellar anionic clay. *Pharm. Res.* **2006** *23*, 604-613.

[28] Costantino, U.; Marmottini, F.; Rocchetti, M.; Vivani, R. New synthetic routes to hydrotalcite-like compounds - Characterisation and properties of the obtained materials. *Eur. J. Inorg. Chem.* **1998** *10*, 1439-1446.

[29] Montgomery D. C. Design and analysis of experiments, 5th edition, Wiley & Sons, New York, 2004, pp. 451-454.

[30] Mnova v.11, Mestrelab Research.

[31] Geppi, M.; Forte, C. The SPORT-NMR software: a tool for determining relaxation times in unresolved NMR spectra. *J. Magn. Reson.* **1999**, *137*, 177–185.

[32] Forte, C.; Geppi, M.; Malvaldi, M.; Mattoli,V. Dynamics of an amorphous polymer by an improved NMR approach based on the simultaneous analysis of ^{1}H and ^{13}C relaxation times. *J. Phys. Chem. B* **2004**, *108*, 10832-10837.

[33] Dejean de la Batie, R.; Laupretre, F.; Monnerie, L. Carbon-13 NMR investigation of local dynamics in bulk polymers at temperature well above the glass transition temperature. 1. Poly(vinyl methyl ether). *Macromolecules* **1988**, *21*, 2045-2052.

[34] Dejean de la Batie, R.; Laupretre, F.; Monnerie, L. Carbon-13 NMR Investigation of Local Dynamics in Bulk Polymers at Temperatures Well above the Glass-Transition Temperature. 3. cis-1,4-Polybutadiene and cis-1,4-Polyisoprene. *Macromolecules* **1989**, *22*, 122-129.

[35] Reichle, W. T. Synthesis of anionic clay minerals (Mixed metal hydroxides, hydrotalcite). S*olid State Ionics.* **1986**, *22*, 135-141.

[36] Miyata, S. Anion-exchange properties of hydrotalcite-like compounds: characterization and properties of the obtained materials. *Clays Clay Miner.* **1983**, *31*, 305-311.

[37] Rojas, R.; Palena, M. C.; Jimenez-Kairuz, A. F.; Manzo, R. H.; Giacomelli, C. E. Modeling drug release from a layered double hydroxide–ibuprofen complex. *Appl. Clay Sci.* **2012**, *62-63*, 15-20.

[38] Zhang, Y.; Grant, D. J. W. Similarity in structures of racemic and enantiomeric ibuprofen sodium dihydrates. *Acta Cryst.* **2005**, *C61*, m435-m438.

[39] Censi, R.; Martena, V.; Hoti, E.; Malaj, L.; Martino, P.; Sodium ibuprofen dihydrate and anhydrous: study of the dehydration and hydration mechanisms. *J. Therm. Anal. Calorim.* **2013**, *111*, 2009-2018.

[40] Geppi, M.; Mollica, G.; Guccione, S.; Pignatello, R.; Veracini, C.A. Molecular properties of Ibuprofen and its solid dispersions with Eudragit RL100 studied by solid-state nuclear magnetic resonance. *Pharm. Res.* **2005**, *22,* 1544-1555.

[41] Sideris, P. J.; Gro Nielsen, U.; Gan, Z.; Grey, C.P. Mg/Al ordering in layered double hydroxides revealed by multinuclear NMR spectroscopy. *Science* **2008**, *321*, 113-117.

[42] Azaïs, T.; Tourné-Péteilh, C.; Aussenac, F.; Baccile, N.; Coelho, C.; Devoisselle, J.-M.; Babonneau, F. Solid-state NMR study of ibuprofen confined in MCM-41 material. *Chem. Mater.* **2006**, *18*, 6382-6390.

[43] Skorupska, E.; Jeziorna, A.; Paluch, P.; Potrzebowzi, M. J. Ibuprofen in mesopores of mobil crystalline material 41 (MCM-41): A deeper undestranding. *Mol. Pharm.* **2014**, *11*, 1512-1519.

[44] VanderHart, D. L.; Earl,W.L.; Garroway, A.N. Resolution in ^{13}C NMR of organic solids using high-power proton decoupling and magic-angle sample spinning. *J. Magn. Reson.* **1981**, *44*, 361-401.

[45] Rothwell, W. P.; Waugh, J. S. Transverse relaxation of dipolar coupled spin systems under rf irradiation: Detecting motions in solids. *J. Chem. Phys.* **1981**, *74*, 2721- 2732.

[46] Brainard, J.R.; Szabo, A. Theory for nuclear magnetic relaxation of probes in anisotropic systems: Application to cholesterol in phospholipid vesicles**.** *Biochemistry* **1981**, *20,* 4618-4628.

[47] Fujiwara, T.; Nagayama, K. The wobbling-in-a-cone analysis of internal motion in macromolecules. *J. Chem. Phys.* **1985**, *83*, 3110-3117.

[48] Pastor, R. W.; Venable, R. M.; Feller, S. E. Lipid bilayers, NMR relaxation, and computer simulations. *Acc. Chem. Res.* **2002**, *35*, 438-446.